Torsional Dynamics and Orientation of DNA−DAPI Complexes†

Maria Luisa Barcellona‡ and Enrico Gratton*,§

Istituto di Chimica Biologica, Università di Catania, Catania, Italy, and Laboratory for Fluorescence Dynamics, University of Illinois at Urbana-Champaign, Urbana, Illinois 61801

Received May 8, 1995; Revised Manuscript Received October 30, 1995⊗

ABSTRACT: The flexibility of calf thymus DNA and several polynucleotides was measured using the anisotropy decay of DAPI bound to DNA, a minor groove probe. DNA torsional dynamics were analyzed using the Schurr model [Allison, S. A., & Schurr, J. M. (1979) *Chem. Phys. 41*, 35−44] in the infinite polymer length approximation. Time-resolved fluorescence depolarization was measured using a frequency-doubled mode-locked dye laser and frequency-domain acquisition methods. At very high P/D ratios, the anisotropy decay is dominated by DNA torsional dynamics. The recovered values of the torsional elastic constant were in good agreement with literature values obtained using other DNA probes. The exact knowledge of the angle between the probe emission dipole transition moment and the helix axis is critical for the determination of the polymer elastic constant. At low P/D ratios, energy transfer between dye molecules strongly contributes to the anisotropy decay. We have developed a statistical model that describes the anisotropy decay, when the correct geometrical factors are included. At low P/D ratios the anisotropy decay is dominated by fluorescence homotransfer. In this regime, it is possible to determine the orientation of the dye molecule with respect to the polymer with accuracy. The values obtained for the distance and orientation of the DAPI molecules in solution using the fluorescence measurements are in excellent agreement with those from the crystal structure of the oligonucleotides−DAPI complex by Dickerson's group [Larsen T. A., Goodsell, D. S., Cascio, D., Grzeskowiak, K., & Dickerson, R. E. (1989) *J. Biomol. Struct. Dyn. 7*, 477−491].

In recent years there has been a renewed interest in DNA dynamics (Allison & Schurr, 1979; Hogan et al., 1979; Thomas et al., 1980; Dickman et al., 1982; Schurr, 1984; Fujimoto et al., 1985; Schurr & Fujimoto, 1988; Mohan & Yathindra, 1991; Kumar et al., 1992; Olson et al., 1993; Kahn et al., 1994). The conformational flexibility and dynamics of the DNA polymer is very complex. DNA can assume different conformations and can exhibit variable electrostatic binding free energy depending on the nature of solvent, temperature, pH, and ligands (Mathieson & Olayemi, 1975; Ott et al., 1975; Record, 1975; Wolf et al., 1975; Avitabile et al., 1980; Masotti et al., 1981; Wilson et al., 1985b; Misra et al., 1994). More interesting are the changes in local conformation that the DNA molecule can undergo upon interaction with proteins (Syvanen, 1975; Burckhardt et al., 1976a,b; Champoux, 1978) and other molecules in a cell (Pullman & Pullman 1981; Dervan, 1986; Zimmer & Waehnert, 1986). The study of DNA conformation and flexibility has been one of the major goals of the physical-chemistry investigation of DNA (Mohan & Yathindra, 1991; Lilley & Clegg, 1993; Eis & Millar, 1993; Kahn et al., 1994). Design and development of sequence-specific DNA binding agents are being actively pursued as probes in molecular biology and as drugs for genetic targeting (Dervan, 1986). Recently, the developments of better models for DNA dynamics (Allison & Schurr, 1979) and the availability of instrumentation with new capabilities (Gratton and Limkeman, 1983a,b; Gratton et al., 1984a,b; Beechem & Gratton, 1988) have offered new possibilities for a better understanding of DNA dynamics. During the past decade, a number of papers by the M. Schurr group have laid the framework for a mathematical description of DNA motions (Thomas et al., 1980; Schurr, 1984; Fujimoto et al., 1985; Schurr et al., 1988). The model used by Schurr assumes that the DNA molecule can be treated as a flexible rod with hydrodynamic properties. In the case of large DNA molecules, in the so-called intermediate region, the solution of the equation of the motion of the flexible rod, given by Schurr, takes a form amenable to data fitting.

During the last decade, a number of new fluorescent probes for DNA and RNA structure and dynamics have appeared. In addition, several DNA dye complexes have been crystallized, and the X-ray structure has been determined (Jain & Sobell, 1984; Pjiura et al., 1987; Ginell et al., 1988; Larsen et al., 1989; Spink et al., 1994). A common probe for DNA studies is DAPI, a minor groove binding probe, and progress has been made toward a better understanding of the modalities of binding for this probe (Kapuscinski & Szer, 1979; Manzini et al., 1983, 1985b; Wilson et al., 1985a, 1989; Szabo et al., 1986; Kubista et al., 1987; Neidle et al., 1987; Strekowski et al., 1989; Hard et al., 1990; Loontiens et al., 1991; Jansen et al., 1993). In particular, we have reached a partial consensus about the photophysical and photochemical deactivation processes for the DNA/DAPI complex (Cavatorta et al., 1985; Barcellona & Gratton, 1991; Tanious et al., 1992).

In this article we report a time-resolved fluorescence depolarization study of DAPI bound to DNA to determine the potential use of such a minor groove binding ligand for probing nucleic acid structure and dynamics (Cooper &

† This work was supported by CNR, Italy (Grant 920426704), by MURST Grant 1992 to M.L.B., and by NIH Grant RR-03155 to E.G.

* Corresponding author.
‡ Università di Catania.
§ University of Illinois at Urbana-Champaign.

⊗ Abstract published in *Advance ACS Abstracts,* December 15, 1995.

0006-2960/96/0435-321$12.00/0

Hagerman, 1990; Clegg et al., 1992). DAPI is a minor groove probe; it binds with high affinity to A-T-A-T sequences, and it is strongly fluorescent when bound to DNA. The quantum yield increases by more than 50 between the bound and unbound form. A large number of thermodynamic and spectroscopic studies have been performed on the DNA−DAPI complex (Kapuscinski & Szer, 1979; Masotti et al., 1981, 1982; Manzini et al., 1983, 1985a; Wilson et al., 1985a, 1989; Szabo et al., 1986; Barcellona et al., 1986; Kubista et al., 1987). It is known that, in addition to binding to AT sites, DAPI can also bind to GC pairs, although with less affinity and without fluorescence enhancement. A number of recent studies have also shown that the fluorescence spectroscopic characteristics of DAPI depends on the DNA sequence (Wilson et al., 1990; Tanious et al., 1992, 1994; Eriksson et al., 1993).

A DNA minor groove binding ligand, such as DAPI, exhibiting antitumor and antitrypanosomal activities, has an interfering role with topoisomerase enzymatic activity. This class of enzymes modulates the topological state of DNA *in vivo*, through a transient double-stranded break. The catalytic reaction requires a high-energy cofactor and occurs by ATP hydrolysis. Members of these, clinically relevant, drugs are defined by their ability to interrupt the breaking/reunion reaction of DNA topoisomerase I by trapping reversible topoisomerase I cleavable complexes (Storl et al., 1993; Megan et al., 1993; Chen et al., 1993). The possibility of monitoring variations in DNA supercoiling, mediated by small organic molecules, is of considerable interest for obtaining information about the determinants of topological changes involved in DNA structural transitions, affecting transcriptional regulatory activity.

Our previous studies were directed to a better spectroscopic characterization of DNA−DAPI complex, and we demonstrated that DNA−DAPI complex microheterogeneity can be detected from the analysis of the fluorescence decay (Barcellona & Gratton, 1989). We attributed the observed fluorescence lifetime distribution for the complex to different binding sites with slightly different environments, sufficient to alter the DAPI fluorescence decay characteristics (Barcellona et al., 1990). The lifetime distribution was very narrow for poly(dA)·poly(dT)/DAPI complex, but the distribution became relatively broad for natural DNA (Barcellona & Gratton, 1989).

In this article we focus on the DNA torsional dynamics. To measure the fluorescence decay, we use frequency-domain methods which are known for their high accuracy and sensitivity (Gratton & Limkeman, 1983a; Gratton et al., 1984b). Recently, a study of DNA flexibility using an intercalating probe, ethidium bromide has been presented, also using the frequency-domain technique to study DNA torsional dynamics (Collini et al., 1992). Although our results agree with some of the observations of this study, we differ in the details of the model used for energy transfer, in the modalities of data analysis, and in some of the important conclusions.

Fluorescence depolarization of intercalating dyes such as ethidium bromide has been extensively used for the study of DNA torsional dynamics. There is a general agreement that the model refined by the group of M. Schurr is the most adequate for the description of the torsional motion. In this model, the analysis of the fluorescence anisotropy decay of DAPI bound to DNA is based on two distinct physical processes: (a) depolarization due to motion of the DNA segment where DAPI resides, and (b) depolarization due to energy transfer to other molecules of DAPI bound in neighboring sites along the DNA molecule. At very high P/D ratio, (P)hosphate to (D)ye, the energy transfer mechanism is negligible and the depolarization is due to DNA torsional motion. At intermediate P/D ratios, a combination of these two effects can be observed. The extent of depolarization due to torsional motion depends critically on the orientation of the DAPI dipole transition moments with respect to the local torsional axis. Due to the nature of the equation describing torsional motion, there is a strong mathematical correlation between the parameter describing the torsional spring constant and the direction of the transition dipole moment of the DAPI molecule with respect to the DNA helical axis. Therefore, it appears that the exact knowledge of the angle is necessary to determine the spring constant. Although the problem of the knowledge of the angle of the transition dipole moment with the helical axis was already noted by previous investigators, for ethidium bromide, it was assumed that this angle was 90° in some of the original work (Paoletti & Le Pecq, 1971) and later corrected to 70.5° (Wu et al., 1991). In principle, for the DNA−DAPI complex in solution this angle is unknown, and, given the direction of the DNA minor groove, a relatively small change in this angle can cause a large variation in the recovered value of the spring constant. However, the modalities of energy transfer critically depend on the orientation and distance between the DAPI molecules along the polymer. By exploiting the energy transfer mechanism we were able to (i) precisely determine the geometry of the binding, (ii) evaluate the spring constant, and (iii) compare our structural results obtained in solution with crystal structures determined using oligonucleotide−DAPI complexes (Larsen et al., 1989). Although this work is not introducing a new method for the analysis of the fluorescence anisotropy decay of dyes bound to DNA, it exploits the effect on fluorescence depolarization due to energy transfer to better determine the geometry of the complex, rather than assuming a particular geometry.

THEORY

Depolarization due to Torsional Dynamics

We used the theory developed by Allison and Schurr (1979) that describes local torsional dynamics using the approximation in which the rotation of the polymer is neglected, i.e., the polymer is very long. The basis of the theory is a model in which the polymer is assumed to be made of beads connected with springs. Only torsional motions of the beads are allowed, and bending motions are ignored. The hydrodynamic model contains, as free parameters, the size of the bead, the torsional constant of the spring joining the beads, and the frictional coefficient. The solution of the motion of the beads is in general very complex. However, in the so-called intermediate zone in which the rotation of the whole molecule is neglected and the ends of the molecule are kept fixed, a closed form solution has been proposed by Thomas et al. (1980). The autocorrelation function of the orientation of a dipole, rigid with respect to a bead, can be written in a form which is relatively simple

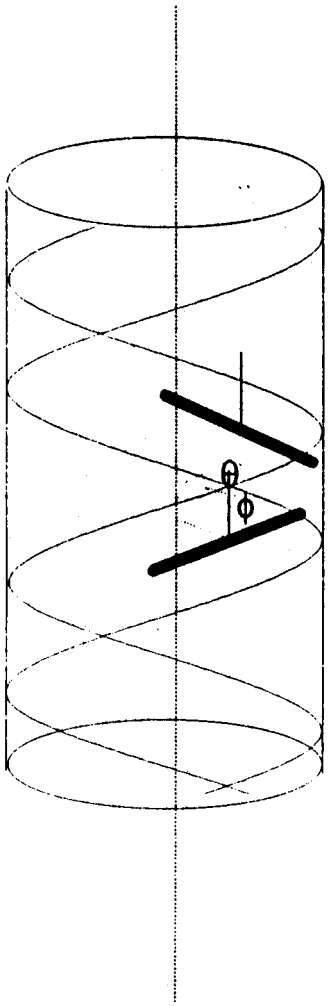

FIGURE 1: Schematic representation of two dye molecules in the DNA minor groove. The angle ϕ is the angle of the dye transition dipole moment with the helical axis. The absorption and emission dipole moments are collinear, and the direction of the transition moment is aligned with the dye molecular axis. The angle θ is the angle between the center of two dye molecules projected on a plane perpendicular to the cylinder axis. The dye molecules are placed tangent to the cylinder surface at 8 Å from the cylinder axis.

and allows for rapid calculations. The basic equation for the anisotropy decay in the time domain is

$$r_b = r_o(A_1 + A_2 e^{-c\sqrt{t}} + A_3 e^{-4c\sqrt{t}})$$

$$c = kT(\pi\gamma K_s)^{-0.5}$$

$$A_1 = (1.5\cos^2\phi - 0.5)^2$$

$$A_2 = 3.0\sin^2\phi\cos^2\phi$$

$$A_3 = 0.75\sin^4\phi \qquad (1)$$

In these expressions, k is the Boltzmann constant (1.38×10^{-16} erg/K), T the absolute temperature, K_s the spring constant in units of dyn cm, $\gamma = 4\pi\eta a^2 h = 5.8 \times 10^{-23}$ dyn cm s, where η is the medium viscosity (1 cp), a the radius of the bead (10 Å), and h the height of the bead (3.4 Å). The angle ϕ is the angle of the transition dipole moment of the fluorophore with the helical axis (Figure 1). These expressions assume that the excitation and emission transition dipole moments are parallel, i.e., $r_o = 0.4$, and that the torsional axis of rotation is coincident with the DNA helical axis. The anisotropy decay expression has been incorporated into the expression for the parallel and perpendicular polarized intensity decay.

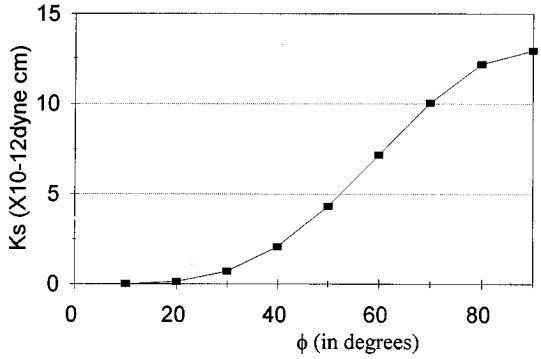

FIGURE 2: Correlation between the spring constant K_s and the angle ϕ. The points were obtained by simulation of the anisotropy decay for $K_s = 5 \times 10^{-12}$ dyn cm and $\phi = 50°$. The data were fit imposing different values for the angle ϕ. All the fits gave reduced χ^2 values that differ by less than 0.07.

$$I(t)_{par} = \frac{I_0}{3}(1 + 2r_b(t))e^{-\Gamma_f t}$$

$$I(t)_{per} = \frac{I_0}{3}(1 - r_b(t))e^{-\Gamma_f t} \qquad (2)$$

where I_o is the excitation intensity and Γ_f is the fluorescence decay rate. These equations have been Fourier transformed in the frequency domain and incorporated into the Globals Unlimited analysis software that allows for a global analysis of all data sets simultaneously (Beechem et al., 1983; Beechem & Gratton, 1988).

To study some properties of the model, we performed a simulation of anisotropy decay curves. In particular we studied the dependence of the anisotropy decay curves on the value of the angle ϕ and of the spring constant K_s. The simulations show that almost identical decay curves can be obtained using different pairs of ϕ and K_s values. To better understand this apparent parameter correlation, we simulated a decay curve with a given value of ϕ and K_s using the above equations for the parallel and perpendicular intensity components. We performed a series of fits of the simulated data imposing different values of the angle ϕ and letting the computer find the value of the spring constant K_s that fits the simulated curve. We have obtained the graph of Figure 2, which reports the values of the K_s parameters as a function of the angle ϕ that gives quasiidentical fits. Since the data are simulated without noise, a perfect fit gives a reduced χ^2 of zero. In the range of angles 20−90°, the χ^2 of the fits was less than 0.07. Since in real measurements this small difference of χ^2 values cannot be appreciated, we concluded that the mathematical correlation between the two parameters ϕ and K_s prevents their independent determination from a single anisotropy decay measurement. This result is independent of the particular DNA−dye complex but only depends on the mathematical nature of the equation describing the depolarization motion. Therefore, all previous studies using the same equation were affected by this correlation. Of course, measurements as a function of temperature or viscosity should only affect the rotational motion of the DNA segment without changing the orientation of the dye, thereby

allowing a separate determination of the two parameters. However, given the very large variation of K_s as a function of ϕ (Figure 2), small variations of the DNA structure due to different solvents or temperature can be wrongly attributed to changes in DNA stiffness.

Depolarization due to Energy Transfer

When the dye coverage of the DNA is relatively large, another mechanism can contribute to depolarization, namely, energy transfer to identical chromophores. Energy transfer between identical molecules do not affect the lifetime of the excited state if all molecules are spectroscopically equivalent, but it can affect the decay of the emission anisotropy. In the case of DAPI bound to DNA, there are at least two different binding modalities, one in which DAPI is bound to AT sites and gives a fluorescent species and a second modality of binding in which DAPI is interacting also with GC pairs and gives a nonfluorescent species (the quantum yield is a factor of about 50 less than the AT-bound species) (Manzini et al., 1983, 1985b; Wilson et al., 1989, 1990; Tanious et al., 1994). The GC-bound species is populated only at very low P/D ratios. In addition, we previously demonstrated that DAPI bound to calf thymus DNA shows fluorescence heterogeneity (Barcellona & Gratton, 1989). Under these conditions, all DAPI molecules are not spectroscopically equivalent. In our analysis we neglected the spectroscopic heterogeneity of DAPI molecules bound to different sites, which is a good approximation for the synthetic polymers experiments but is not sufficient for the calf thymus DNA experiments. In addition, due to the AT/GC ratio of calf thymus DNA and the random distribution of the AT triplets, the effect of transfer cannot be treated exactly for natural DNAs.

Förster (1951) has derived the basic formulas that describe nonradiative rate of energy transfer $\Gamma_{d,a}$ in the weak coupling approximation.

$$\Gamma_{d,a} = \Gamma_d\left(\frac{R_0}{d}\right)^6$$

$$R_0{}^6 = \frac{\kappa^2 K_T}{\Gamma_d}$$

$$\kappa^2 = (\cos\theta_{12} - 3\cos\vartheta_1\cos\vartheta_2)^2 \qquad (3)$$

Γ_d is the decay rate of the donor in the absence of acceptor. The κ^2 factor depends on the relative orientation of the donor−acceptor transition dipole moments, where θ_{12} is the angle between the direction of the two transition dipole moments and θ_1 and θ_2 the angles of the two dipoles with the line joining the centers of the dipoles. The rate K_T depends on the superposition integral and on the medium refractive index (Förster, 1951), and d is the distance between donor and acceptor. The distance d and the κ^2 factor have been calculated in terms of the relative position of the donor−acceptor pair along the DNA molecule and the distance of the center of the dye molecule from the helical axis (8 Å).

$$d = \sqrt{2r^2(1-\cos\vartheta) + l^2}$$

$$\cos\vartheta_{12} = \sin^2\phi\cos\vartheta + \cos^2\varphi$$

$$\cos\vartheta_1 = \frac{r}{d}\sin\vartheta\cos\varphi + \frac{l}{d}\cos\varphi$$

$$\cos\vartheta_2 = \frac{r}{d}\sin\vartheta(\cos\vartheta - 1) + \frac{r}{d}\sin\vartheta\cos\vartheta\sin\varphi + \frac{l}{d}\cos\varphi \qquad (4)$$

where the angle ϕ is the angle with the helical axis already defined, θ is the rotation angle for n bases movement (multiple of 36°), and l the distance between n base along the helical axis (multiple of 3.4 Å).

The expressions for the decay of the intensity parallel and perpendicular to the excitation direction in the presence of energy transfer between a pair of identical chromophores are the following

$$I\left(t\right)_{par} = \frac{I_0}{3}\left(1 + r_{01}(1 + e^{-K_T t}) + r_{02}(1 - e^{-K_T t})\right)e^{-\Gamma_f t}$$

$$I(t)_{per} = \frac{I_0}{3}\left(1 - \frac{r_{01}}{2}(1 + e^{-K_T t}) - \frac{r_{02}}{2}(1 - e^{-K_T t})\right)e^{-\Gamma_f t} \qquad (5)$$

where r_{01} is the anisotropy decay of the donor only and r_{02} that of the acceptor only. We have assumed that the anisotropy of the acceptor is equal of that of the donor multiplied by a factor that accounts for the different orientation of the transition dipole moment of the acceptor. This factor depends on the relative location of the acceptor relative to the donor along the DNA molecule and it must be evaluated for each donor−acceptor pair.

$$r_{02} = r_{01}\frac{3\cos^2\vartheta_{12} - 1}{2} \qquad (6)$$

where θ_{12} is the angle between donor and acceptor previously defined. Due to the particular geometry of the DAPI molecules along the DNA helix, the equation for the depolarization due to energy transfer contains only two variables, i.e., the angle between donor and acceptor and the rate of transfer. The angle between donor and acceptor can only take discrete values, depending on the location of the acceptor relative to the donor on the DNA molecule. The transfer rate depends on several factors. Therefore, to apply Förster theory to the particular case of DAPI bound to DNA, we need to evaluate the distance between DAPI molecules, the relative orientation between the transition dipole moments, the overlap integral, and other parameters such as the index of refraction. The distance distribution between DAPI molecules along the DNA is dependent on both geometrical constraints and the stoichiometry of binding. In our analysis, we have allowed to change the orientation of the DAPI molecule with respect to the helical axis (angle ϕ). In addition, we assumed that each DAPI molecule occupies three consecutive bases. Given the charges on the DAPI molecule, it has been suggested that the minimum distance between two DAPI molecules should be four base pairs. The fit of the experimental data has been carried out under these two assumptions, i.e., a minimum distance of three or four bases between DAPI molecules. It is unclear if, at the shortest distances, Förster theory can be applicable, due to the quasicontact between the two DAPI molecules. In our derivation, we have assumed that the DAPI molecule is placed tangent to a cylinder coaxial with the polymer at a

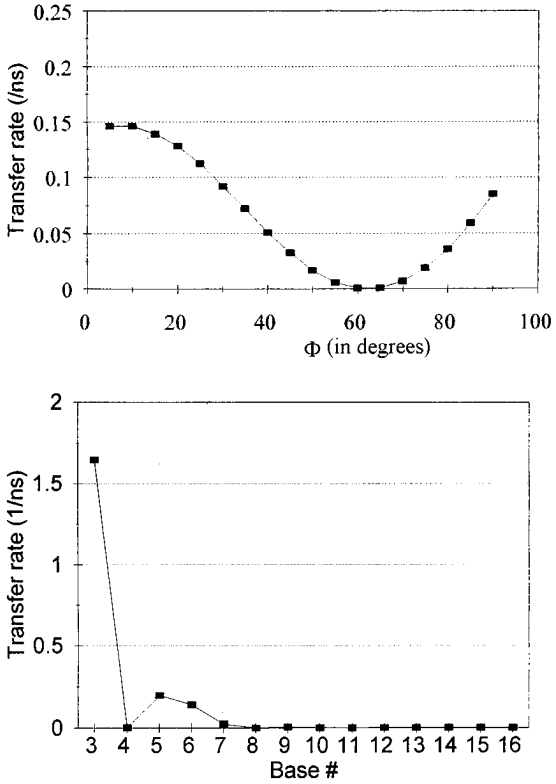

FIGURE 3: (a, top) Energy transfer rate as a function of the angle ϕ. The acceptor molecule is placed four bases away in the geometry shown in Figure 1. (b, bottom) Energy transfer rate as a function of the position of the acceptor along the DNA molecule. For this figure the angle ϕ is 62°. All the other parameters for the calculation of the transfer rate are described in the text.

distance of 8 Å from the helical axis (Kubista et al., 1987). Under these assumptions, only one angle, the angle ϕ, is sufficient to determine the orientation of the DAPI molecule, i.e., the angle with the cylinder axis (Figure 1). Also we have assumed that the transition dipole moment is coincident with the long molecular axis of DAPI which includes the indole fluorescent moiety (Kubista et al., 1988; Clegg et al., 1993; Eriksson et al., 1993; Jansen et al., 1993). Given the above geometry, we can now sequentially place DAPI molecules along the DNA double helix and calculate the relative contribution to transfer of an acceptor DAPI molecules distant 1, 2, ..., n. bases from the donor DAPI molecule. Given the κ^2 factor and the sixth power dependence of the rate of transfer on the distance, we obtain a distribution of transfer efficiencies along the chain with a broad minimum around an angle ϕ of 62° when donor and acceptor are four bases apart (Figure 3a). This effect is due to the structure of the B-form of DNA that has 10 bases per turn. At a distance of 4, 8, and 12 bases we have a relative orientation between DAPI molecules that gives a κ^2 factor of about zero if the angle ϕ is 62° (Figure 3b). If the minimum distance between two DAPI molecules is four bases, for adjacent molecules, energy transfer can be minimal due to the combination of the ϕ and of the θ angles. At other locations the transfer efficiency can be larger if the typical transfer distance R_o is larger than 20.4 Å (minimum distance between DAPI molecules placed four bases apart), since the transition dipole moments are more favorably oriented for energy transfer. The characteristic distance R_o can be obtained from the overlap integral and the fluorescence quantum yield. The overlap integral was calculated from the absorption and emission spectrum of DAPI bound

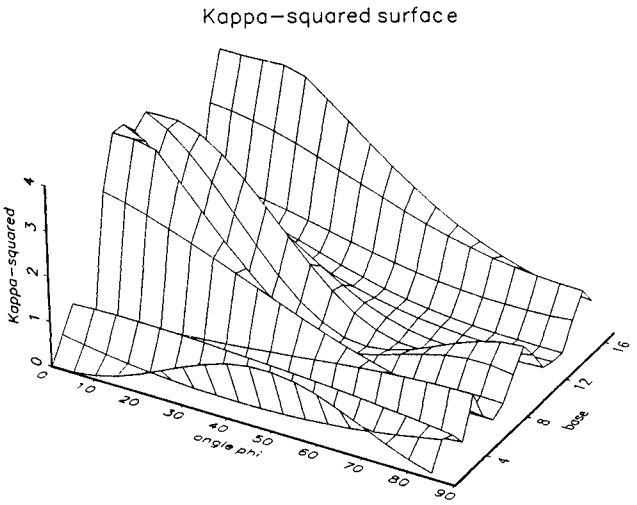

FIGURE 4: κ^2 surface for acceptors located at different base distances as a function of the angle ϕ of the dye molecule with respect to the helical axis.

to DNA using well known expressions [see, for example, Lakowicz (1986)]. The value of R_o resulted about 21.4 Å using 1.7 for the index of refraction. The quantum yield was evaluated from a measurement of the decay rate. As shown in Figure 4, the κ^2 factor that enters in the transfer efficiency equation is a complex function of the angle ϕ and of the position of the acceptor along the DNA. The simultaneous effect of depolarization due to energy transfer and torsional motion was treated according to Wu et al. (1991).

Binding Statistics

The effective occupation of a particular DNA site is determined by the binding statistics. The amount of binding and the relative location of bound molecules is dependent upon the binding affinity of a single dye molecule and upon the cooperativity parameter. McGhee and von Hippel (1974) have derived general formulas for the distribution of gap lengths in DNA under general conditions. We have used a combinatorial approach similar to that proposed by McGhee and von Hippel to calculate the average number and location of sites occupied by DAPI on the DNA. However, the McGhee−von Hippel formulas cannot be directly applied to the energy transfer distance distribution since for energy transfer we must evaluate the probability of finding a particular distribution of acceptors on both sides of an occupied site. The two problems, i.e., the distribution of gap lengths and the distribution of molecules at the distance of 3, 4, 5, ..., i bases apart, are related. We have followed the same basic idea, used by McGhee and von Hippel for the calculation of the distribution of gap lengths, to calculate the statistical distribution of acceptors, which is relevant for energy transfer. We have assumed no cooperativity of binding, a reasonable assumption for DAPI, and that all sites were available for binding of the dye. Of course, for calf thymus DNA the AT/GC ratio determines that all sites are not available for DAPI binding. The probability of finding an acceptor dye molecule at a given location from the donor dye molecule for the polymers can be obtained in the following manner. First, consider only one side of the DNA molecule relative to a site already occupied. Assume that the dye molecule can occupy n consecutive bases. Clearly, the first acceptor must be at least n bases apart. If a is the

Table 1: Probability of Finding an Acceptor at Different Positions along the dna Double Helix

(a) Dye molecule Occupies Two Bases

$P(1) = 0$
$P(2) = a$
$P(3) = a(1 - a)$
$P(4) = a[(1 - a)^2 + a]$
$P(5) = a[(1 - a)^3 + 2a(1 - a)]$
$P(6) = a[(1 - a)^4 + 3a(1 - a)^2 + a^2]$
$P(7) = a[(1 - a)^5 + 4a(1 - a)^3 + 3a^2(1 - a)]$
$P(8) = a[(1 - a)^6 + 5a(1 - a)^4 + 6a^2(1 - a)^2 + a^3]$
$P(9) = a[(1 - a)^7 + 6a(1 - a)^5 + 10a^2(1 - a)^3 + 4a^3(1 - a)]$
$P(10) = a[(1 - a)^8 + 7a(1 - a)^6 + 15a^2(1 - a)^4 + 10a^3(1 - a)^2 + a^4]$
$P(11) = a[(1 - a)^9 + 8a(1 - a)^7 + 21a^2(1 - a)^5 + 20a^3(1 - a)^3 + 5a^4(1 - a)]$
$P(12) = a[(1 - a)^{10} + 9a(1 - a)^8 + 28a^2(1 - a)^6 + 35a^3(1 - a)^4 + 15a^4(1 - a)^2 + a5]$
$P(13) = a[(1 - a)^{11} + 10a(1 - a)^9 + 36a^2(1 - a)^7 + 56a^3(1 - a)^5 + 35a^4(1 - a)^3 + 6a^5(1 - a)]$
$P(14) = a[(1 - a)^{12} + 11a(1 - a)^{10} + 45a^2(1 - a)^8 + 84a^3(1 - a)^6 + 70a^4(1 - a)^4 + 21a^5(1 - a)^2 + a^6]$
$P(15) = a[(1 - a)^{13} + 12a(1 - a)^{11} + 55a^2(1 - a)^9 + 120a^3(1 - a)^7 + 126a^4(1 - a)^5 + 56a^5(1 - a)^2 + 7a^6]$
etc...

(b) Dye Molecule Occupies Three Bases

$P(1) = P(2) = 0$
$P(3) = a$
$P(4) = a(1 - a)$
$P(5) = a(1 - a)^2$
$P(6) = a[(1 - a)^3 + a]$
$P(7) = a[(1 - a)^4 + 2a(1 - a)]$
$P(8) = a[(1 - a)^5 + 3a(1 - a)^2]$
$P(9) = a[(1 - a)^6 + 4a(1 - a)^3 + a^2]$
$P(10) = a[(1 - a)^7 + 5a(1 - a)^4 + 3a^2(1 - a)]$
$P(11) = a[(1 - a)^8 + 6a(1 - a)^5 + 6a^2(1 - a)^2]$
$P(12) = a[(1 - a)^9 + 7a(1 - a)^6 + 10a^2(1 - a)^3 + a^3]$
$P(13) = a[(1 - a)^{10} + 8a(1 - a)^7 + 15a^2(1 - a)^4 + 4a^3(1 - a)]$
$P(14) = a[(1 - a)^{11} + 9a(1 - a)^8 + 21a^2(1 - a)^5 + 10a^3(1 - a)^2]$
$P(15) = a[(1 - a)^{12} + 10a(1 - a)^9 + 28a^2(1 - a)^6 + 20a^3(1 - a)^3 + a^4]$
etc...

(c) Dye Molecule Occupies Four Bases

$P(1) = P(2) = P(2) = 0$
$P(4) = a$
$P(5) = a(1 - a)$
$P(6) = a(1 - a)^2$
$P(7) = a(1 - a)^3$
$P(8) = a[(1 - a)^4 + 1a(1 - a)]$
$P(9) = a[(1 - a)^5 + 2a(1 - a)^2]$
$P(10) = a[(1 - a)^6 + 3a(1 - a)^3]$
$P(11) = a[(1 - a)^7 + 4a(1 - a)^4 + a^2]$
$P(12) = a[(1 - a)^8 + 5a(1 - a)^5 + 3a^2(1 - a)^2]$
$P(13) = a[(1 - a)^9 + 6a(1 - a)^6 + 6a^2(1 - a)^3]$
$P(14) = a[(1 - a)^{10} + 7a(1 - a)^7 + 10a^2(1 - a)^4]$
$P(15) = a[(1 - a)^{11} + 8a(1 - a)^8 + 15a^2(1 - a)^5 + a^3]$
etc...

probability of base occupation, then the probability to find an acceptor in the first available position is a. The probability to occupy the second available position is $a(1 - a)$, and the third is $a(1 - a)^2$. This series continues until the number of sites between donor and acceptor is equal to or larger than the number of positions occupied by the dye molecule. For larger distances, we need to add the probability that a dye molecule occupies a site between the acceptor and the donor. If the distance is equal to the length occupied by the dye, this probability is a. If the distance is one position longer, then this probability is $2a(1 - a)$, since there are two possible combinations of the dye molecule in that gap. The series continues with terms of the kind $ia(1 - a)^{i-1}$ until two dye molecules can be interposed in the gap between donor and acceptor. At this point an extra term must be added. For the occupation probability of a site at a distance i (bases apart) from a site already occupied, we have found the following series given in Table 1 if the number of bases occupied by a dye molecule is two, three, and four. Similar series can be written using the same combinatorial principle if the dye molecule occupies five or more sites along the DNA molecule. Clearly, the probability of finding an acceptor on the other side of the DNA molecule is the same for both sides. The value of the single site probability, a, can be calculated using the binding constant for the complex DAPI−DNA and the concentrations of both DAPI and DNA.

When the probability of site occupation is large, the series of Table 1 have an oscillatory kind of behavior since acceptors can only be at a distance n bases apart if every site is occupied. The oscillatory behavior persists also for lower occupation probability. Figure 5 shows the probability of finding a dye molecule at a distance i bases apart as a function of DNA coverage for the case $n = 4$.

We note that our expression for the probability of a donor at a given distance from an acceptor is different from that used by Collini et al. (1992) for the calculation of the distance distribution of dye molecules in their study of energy transfer of ethidium bromide bound to DNA. These authors have used the formula of McGhee and von Hippel (1974), without modification for the energy transfer case. However, contrary to the experiments reported here, in their experiments the energy transfer term was giving a small contribution to the overall anisotropy decay.

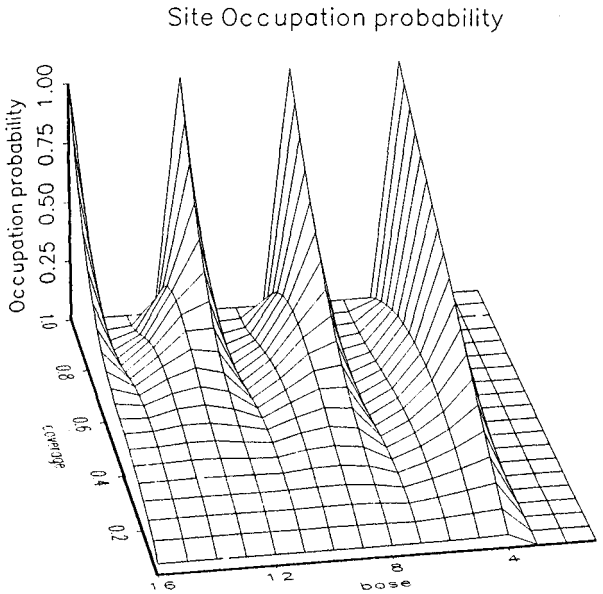

FIGURE 5: Site occupation probability as a function of DNA coverage. For this simulation it was assumed that dye molecules can be placed only four bases apart. A similar surface is obtained if dye molecules can be placed three bases apart.

The knowledge of the probability of each site to be occupied and of the transfer rate to each individual site is not sufficient to evaluate the rate of transfer to one particular acceptor. The rate of transfer depends on the overall configuration of acceptors around a donor and not only on the presence of one particular acceptor. Therefore, we need to evaluate, for each configuration reported in Table 1, the transfer rate of that configuration and the probability of the energy transfer to one particular acceptor of the configuration. For example, consider the row denoted by P(12) of Table 1a. There are five different ways a dye molecule can be interposed in the gap between donor and acceptor and three different ways that two dye molecules can be interposed. For each of these configurations we must calculate the transfer rate and the relative probability that the energy ends up in one of the possible acceptors. This calculation is automatically performed by the fitting program for each DNA coverage and as a function of the transfer rate. As an example, Figure 6 reports the distribution of transfer rates and the distribution of emitting acceptors for one particular value of the angle $\phi = 50°$ and for a single site occupation probability of 0.5. The anisotropy decay function used for the fit in our work accounts for (i) energy transfer up to 12 bases apart, (ii) the average donor site occupation, given a DNA and DAPI concentration, based on the binding constant reported in the literature, and (iii) the rate distribution, as provided by the combinatorial series reported above.

We have also evaluated the effect of multiple sequential transfer. The following discussion is partially based on the experimental finding that the minimum base distance between DAPI molecules found in our work is three. In general, due to the particular dependence of the energy transfer equation on next neighbor distance, multiple transfer, i.e., from molecule 1 to molecule 2 and then from 2 to 3 is more efficient than a single transfer from molecule 1 to molecule 3. We have neglected higher order terms in the energy transfer expression at relatively high P/D ratio. However, at low P/D ratio, multiple transfer can be very efficient. We have performed a simulation using a Monte Carlo method to determine the extent of multiple transfer. This method

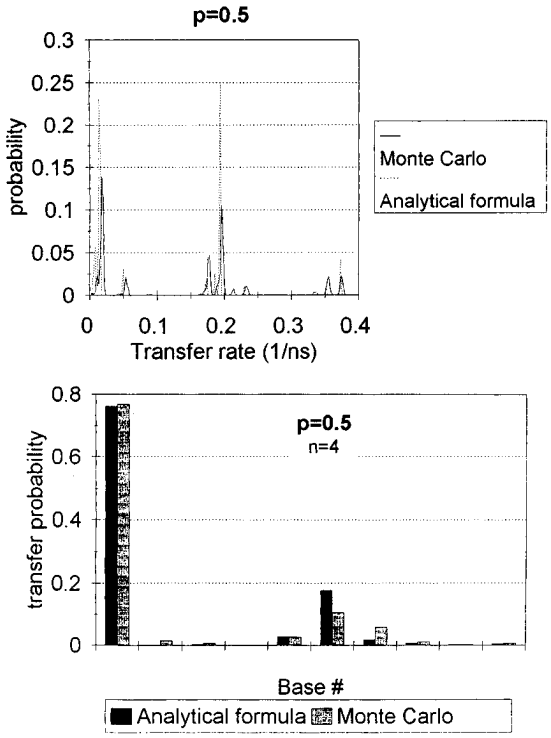

FIGURE 6: Effect of multiple transfer: (a, top) Comparison between the distribution of transfer rates obtained using the analytical formula (broken line) and the Monte Carlo method (solid line) described in the text. (b, bottom) Comparison between transfer probability calculated using the analytical formula for transfer to a single location and as obtained using the Monte Carlo method that allows for multiple transfer. The result of the Monte Carlo method gives a broader distribution of emitters at different locations. This calculation was performed for a fractional DNA coverage of 0.5 and assuming that dye molecules can only be placed at a minimum distance of four bases apart. The angle ϕ was 50°. Emission from bases more than 10 bases apart was considered modulo 10, since this emission is equivalent from the anisotropy point of view.

follows the lines of previous models (Paoletti & Le Pecq, 1971) but adapted to the DNA/DAPI complex. As a result of the simulation, we have obtained the probability distribution of multiple transfer, the distribution of emitting molecules a distance *i* apart from the donor and the distribution of transfer rates (Figure 6). The results of the simulation critically depend on the angle ϕ and on DNA coverage. However, some general results can be established. For calf thymus DNA, the extent of multiple transfer is negligible under all coverage conditions. For the AT polymers, multiple transfer occurs for P/D ratios below 10.

The dependence of transfer efficiency upon DNA coverage has a peculiar behavior for $n = 4$. The transfer efficiency first increases as the coverage increases, reaches a maximum and then decreases at very high coverage (Figure 7). To understand this behavior, consider the limiting case in which the DNA is fully covered. In this situation transfer is minimal, since DAPI molecules are placed at positions 4, 8, 12, etc. along the DNA helix. From the graph of Figure 2, if the angle ϕ is between 40° and about 80°, transfer efficiencies are very small for four bases distance between DAPI molecules. The reason for this decrease is the impossibility of configurations with less than four gaps. The observation of transfer efficiency at high coverage can help to clarify the problem of the number of bases occupied by one DAPI molecule on the DNA. The failure to observe a decrease of transfer efficiency at high DNA coverage (see Results) suggests that DAPI molecules are placed every three

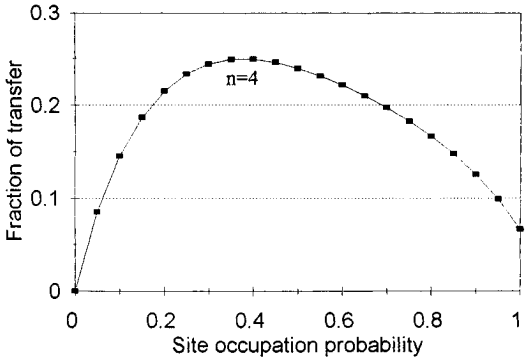

FIGURE 7: Fraction of fluorophores that perform energy transfer as a function of the single site occupation probability. This graph was calculated assuming that dye molecules can be placed at a minimum of four bases apart. The angle ϕ was 50°.

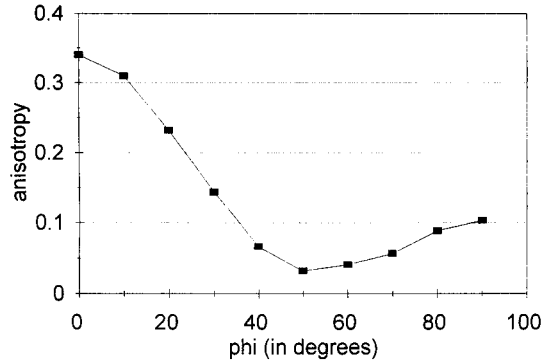

FIGURE 8: Steady-state anisotropy as a function of the angle ϕ. This graph was calculated using the Monte Carlo approach described in the text, assuming full DNA coverage and allowing for multiple transfer.

bases rather than every four as previously suggested (Eriksson et al., 1993).

At full DNA coverage, and in the presence of multiple transfer, the emission occurs from a stretch of the DNA molecule that we have estimated to be about 20−30 bases long using the Monte Carlo approach. The angle ϕ of the DAPI transition dipole moment about the helical axis determines the value of the limiting (r_∞) anisotropy. DAPI molecules appear to be placed on the surface of a cone that provides an "order" to the emission. The cone aperture (the angle ϕ) determines the r_∞ value and also the steady-state anisotropy value. Figure 8 shows the value of the steady-state anisotropy as a function of the angle ϕ obtained using the Monte Carlo approach that allows for multiple transfer. If multiple transfer is not allowed, the steady-state anisotropy never decreases below 0.2, a value incompatible with the experimental results.

Comments on the Approximation Used To Calculate Depolarization due to Energy Transfer

(1) Neglect Transfer to DAPI Bound to GC Pairs. Since this transfer occurs to an essentially dark species, this transfer does not affect the anisotropy decay *per se*. Of course, transfer to DAPI bound to GC pairs can reduce the average lifetime which in turn decreases the effect of depolarization due to transfer. In the case of the polymer data, this transfer cannot occur.

(2) Neglect Cooperativity of Binding. Relatively low cooperativity coefficients have been reported for DAPI bound to DNA (Eriksson et al., 1993). In principle, the number of next neighbors can be larger than that estimated by our formulas. The net effect of neglecting cooperativity will be an erroneous estimation of the number of sites responsible for depolarization due to transfer.

(3) Neglect Local Rotational Diffusion of the DNA Segment in the Expression for the Rate of Energy Transfer. The energy transfer expression considers transfer to fixed locations, neglecting local differences between the dye orientation. In addition, diffusional motions during the excited state are not included. Local flexibility should increase transfer at small distances. On the basis of the high P/D ratio data, when only rotational diffusion caused depolarization, we estimated that the average rotation angle between adjacent sites is relatively small. The DNA molecule rotates as a semirigid cylinder, and although the average rotation of the DAPI molecule is relatively large, the differential rotation with respect to the next site is only a few degrees (Schurr, 1984; Wu et al., 1991).

(4) Neglect DNA Bending. Under our experimental conditions DNA persistence length should be at least 50 nm or longer (Olson et al., 1993). Since transfer is efficient only over few helical turns (at low P/D ratio), bending of the helical axis has a minor effect on the rate of energy transfer. Instead, bending of the DNA molecule causes an additional depolarization effect whose magnitude depends on the value of the persistence length (Wu et al., 1991). Following the estimation of Wu et al. adapted to the case of the DAPI/DNA complex, up to P/D ratios of about 5, when multiple transfer starts to appear, the correction on the recovered torsional constant should less than 20%. At lower P/D ratios, the correction can be substantial. However, we note that in our approach the torsional constant is derived for the limit of low DNA coverage, when energy transfer is negligible. As a consequence, the effect of DNA bending will be reflected in a deviation of the experimental fit only at very low P/D ratio.

(5) Treatment of the Multiple Transfer. Our Monte Carlo simulations have indicated that multiple transfer is quite efficient at low P/D ratio for the polymer. To better establish the influence of multiple transfer on the polarization decay, we have calculated the distribution of emitting molecules and the transfer rate distribution with and without multiple transfer (Figure 6). The only factors affecting the anisotropy decay expression are the angle between donor and final emitter and the rate of transfer to the final emitter. What happens in the intermediate steps is irrelevant. Although the distribution of emitters is different when multiple transfer is allowed, the distribution of emitter angles is not. This effect is due to the periodicity of the angle between donor acceptors after one turn of the DNA helix. Essentially all possible angles are populated without multiple transfer at low P/D ratio, i.e., at the concentration at which multiple transfer can occur. Therefore, multiple transfer has a relatively modest effect on the distribution of emitter orientations, except for the effect of bending discussed at point 4. Also, the distribution of transfer rates is relatively unaffected by multiple transfer (Figure 6a). The formulas for depolarization due to transfer between an isolated donor−acceptor pair cannot give greater depolarization than the average value of the intrinsic anisotropy of the donor and of the acceptor. If the transfer rate is very large, both donor and acceptor have the same emission probability. To account for multiple transfer, we have modified the equation for depolarization due to transfer between an isolated pair in such a way that the energy can only flow from the donor to

the acceptor. Essentially, we have used eqs 2 instead of 5 in which the apparent rotational rate has been substituted with the rate of transfer. This modified equation was used to fit the data point at the lowest P/D ratio. For all other P/D values, the equation given in the text was used.

MATERIALS AND METHODS

4′,6-Diamidino-2-phenylindole dihydrochloride (DAPI) was obtained from Boehringer Mannheim and checked for purity by thin layer chromatography. Calf thymus DNA (58% AT, type I) was also obtained from Boehringer Mannheim. The molecular weight determined by sedimentation resulted about 1.3×10^7, and the preparation was homogeneous. ColE$_1$ plasmid DNA (47% AT), isolated from host strain *Escherichia coli* C$_{600}$, molecular mass equal to 4.2×10^6 Da, was purchased by Sigma Chemical Co. The absorption ratio A_{260}/A_{280} was 1.8. Poly(dA-dT)·poly(dA-dT) and poly(dA)·poly(dT) were from Pharmacia P-L Biochemicals. The average molecular weight of the double-stranded polymers, either self-complementary or alternating, was about 6×10^5, and the polymers homogeneous in molecular weight and conformation as determined by agarose gel electrophoresis in TAE buffer. All DNA samples were used without further purification. All measurements, unless otherwise stated, were performed in the following buffer: 0.1 M Tris-HCl, 0.1 M NaCl, and 0.01 M EDTA, pH 7.4. All reagents dissolved in aqueous buffer solution were of the highest purity available. Steady-state fluorescence spectra of DAPI were performed at 460 and 340 nm, for the emission and the excitation, respectively, on the ISS (ISS Inc., Champaign, IL) photon counting spectrofluorometer, at the Laboratory for Fluorescence Dynamics at the University of Illinois at Urbana-Champaign. Steady-state polarization measurements of DAPI complexed with DNA and with polydeoxynucleotides are previously reported (Barcellona & Gratton, 1993). r_o values were obtained from polarization measurements in propylene glycol at −20 °C.

Anisotropy decay measurements were obtained on the multifrequency phase and modulation fluorometer described by Gratton and Limkeman (1983a), equipped with an ISS1ADC interface (ISS, Champaign, Illinois) for data acquisition and analysis. The excitation source was a HeCd laser (Liconix model 4240 N), using the line at 325 nm. In each experiment, a set of 10−20 different modulation frequencies were employed in the range 10−200 MHz. The emission polarizer was automatically alternated between vertical and horizontal orientations for the measurement of anisotropy decays. Donor/acceptor emission was monitored at 460 and 450 nm for dye molecule alone and complexed with polydeoxynucleotides, respectively. The critical transfer distance R_o was determined from the spectral properties of the chromophore according to the Förster equation, as previously stated. Solution concentrations were determined spectrophotometrically using the following molar extinction coefficients: DAPI in buffer solution $\epsilon = 23\,000$ M^{-1} cm^{-1} at 342 nm, for the polydeoxynucleotides in homopolymers and alternating copolymer sequences were 6000 and 6600 M^{-1} cm^{-1}, respectively. All measurements were carried out at 20 °C using a circulating water bath. To obtain the desired P(Phosphate)/D(Dye) ratio, the final concentration was reached by adding increasing amounts of polymer. Constancy of DAPI concentration was achieved by adding polymer solution containing DAPI at the same molarity as that of the initial, polymer free, solution (6.5×10^{-5} M). In all experiments each sample was allowed to equilibrate at room temperature for at least 5 min before measurement.

Table 2: Flexible Rod Model Analysis: Poly(dA)·Poly(dT)[a]

r_0 (linked)	ϕ (linked) (deg)	K_s (fixed) (dyne × cm) × 10^{-12}	P/D	τ_1 (ns)	f_1	τ_2 (ns)	χ^2
0.32	45	5.7	205	4.00	1.00		0.81
0.32	45	5.7	105	4.00	1.00		0.61
0.32	45	5.7	62	4.00	1.00		0.59
0.32	45	5.7	41	4.00	1.00		0.98
0.32	45	5.7	12	3.97	0.99	0.97	1.31
0.32	45	5.7	10	3.97	0.98	0.53	0.89
0.17[b]	45	5.7	2	3.74	0.95	0.02	1.27

r_0	ϕ (linked) (deg)	K_s (dyne cm) × 10^{-12}	P/D	τ (ns)	χ^2
0.322	45	7.0	205	4.00	0.42
0.323	45	5.8	105	4.00	0.41
0.323	45	4.7	62	4.00	0.53
0.355	45	5.1	41	4.00	0.64

[a] r_0, initial anisotropy; ϕ, angle of the DAPI transition dipole moment with the helical axis; K_s, rotational spring constant; P/D, phosphate to dye ratio; τ_1, long lifetime component; f_1, fractional contribution of the long lifetime component; τ_2, short lifetime component; χ^2, reduced chi-squared. [b] Data set analyzed with a different equation for the energy transfer.

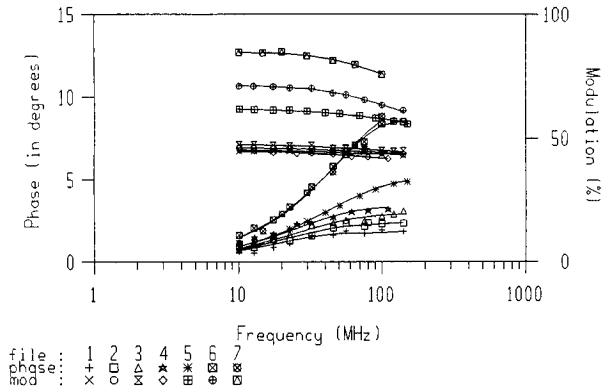

FIGURE 9: Result of the fit of the phase and modulation data using the flexible rod model and the energy transfer expressions for poly(dA)·poly(dT): (1) P/D = 205, (2) P/D = 105, (3) P/D = 62, (4) P/D = 41, (5) P/D = 12, (6) P/D = 10, (7) P/D = 2.

RESULTS

(a) Polydeoxynucleotides. Poly(dA)·poly(dT)/DAPI complexes were studied in P/D range from about 200 to about 2. The fluorescence intensity decay was analyzed using two alternative models. At high P/D ratio, the intensity decay is well described by a single-exponential component with a decay rate of approximately 4.0 ns. As the dye concentration increases, the decay becomes more heterogeneous as previously reported (Barcellona & Gratton, 1989). The second lifetime component, due to the free dye, gives a relatively small contribution to the total fluorescence, except at the lowest P/D ratio, and it was neglected in the analysis of the anisotropy decay. The anisotropy decay was analyzed using the flexible rod model with the additional energy transfer term described under Theory (Table 2a and Figure 9) and using two apparent rotational correlation times (Table 3). The two-rotational component fit gives a global χ^2 of about 1.4, indicating that overall the fit is relatively good. However, the fit is good only at high P/D ratios. It is worth noting that, apparently, two rotational components are sufficient to describe the data. Using this empirical model, at high P/D ratios, the long rotational component should be

Table 3: Two-Rotational Correlation Time Model Analysis: Poly(dA)·Poly(dT)

r_0 (linked)	τ_{1corr} (ns) (linked)	fraction 1	τ_{2corr} (ns)	P/D	χ^2
0.37	0.192	0.196	84.5	205	0.71
0.37	0.192	0.208	58.9	105	0.53
0.37	0.192	0.227	45.6	62	0.26
0.37	0.192	0.146	35.2	41	1.00
0.37	0.192	0.495	26.9	12	2.35
0.37	0.192	0.555	7.1	10	3.21
0.37	0.192	0.737	3.4	2	1.60

associated with the motion of the DNA segment on which DAPI is bound, while the short component might be associated with some local motion of the probe. The data show that the long component progressively decreases in value as the DNA is covered with more dye. This effect is due to the increase of the energy transfer mechanism, rather than to an increase of the rotational correlation time. However, this empirical fit provides some useful information. We have determined that the transfer rate is much faster than the rotational rate of the DNA segment and that, at high DNA coverage, energy transfer is the major depolarization mechanism. Of course, this empirical model cannot provide information about the orientation of the dye molecule with respect to the DNA. In the global fit using the flexible rod model with energy transfer (Table 2a), the only variable parameter was the angle ϕ that was linked among all the data sets. The other parameters where fixed during the fit as shown in the table. The global χ^2 for this fit is less than 1. This result is quite satisfactory indicating that, overall, the model fits the data. For this kind of linked-parameter fit, the total number of free parameters is 1. We also studied whether the parameters of the system such as the torsional force constant and the angle of the transition dipole moment with respect to the helical axis can be considered independent of the P/D concentration. It is well established that several binding modalities are present in the DAPI/DNA complex and that, at very low P/D ratio, at least a second binding modality is occurring in which DAPI interacts with the phosphates (Barcellona et al., 1986; Wilson et al., 1989; Tanious et al., 1994). Based on this consideration, a separate fit was attempted in which the value of the torsional constant and of the intrinsic anisotropy, r_0, was allowed to vary between experiments (Table 2b). Of course, due to the increased number of fitting parameters, this fit gives lower χ^2 values, but still comparable to the linked parameter fit presented in Table 2a. However, we noticed no particular trend in the parameter values as a function of the P/D ratio, which suggests that the linked-parameter fit in which r_0, ϕ and K_s are held constant among the data sets is compatible with the experimental data.

In Table 2a, the recovered value of r_0 for the data set at P/D = 2 is 0.17, well below the expected value for excitation at 325 nm, which is 0.32. We recall that this data set is strongly affected by the presence of free dye. From the stoichiometry of binding, presumably half of the molecules are free in solution. We believe that part of the reason for the reduced value of r_0 is due to the free dye, i.e., the anisotropy of the free dye is about 0.2. Another unaccounted contribution to depolarization comes from multiple transfer, which is only partially simulated for this data set by modification of the energy transfer equation, as described under Theory.

The data fit using the flexible rod model with energy transfer for the heteropolymer poly(dA-dT)·poly(dA-dT) is reported in Table 3. For this polymer, only data at relatively high P/D ratios were analyzed. Using the same angle ϕ obtained for the homopolymer, the value of the elastic spring constant is smaller with respect to the homopolymer, i.e., this polymer appears more flexible.

Table 4: Flexible Rod Model Analysis: Poly(dA-dT)·Poly(dA-dT)

r_0 (linked)	ϕ (linked) (deg)	K_s (fixed) (dyne cm) $\times 10^{-12}$	P/D	τ (ns)	χ^2
0.328	45	2.0	90	4.00	0.66
0.322	45	1.7	40	4.00	0.61

Table 5: Flexible Rod Model Analysis: Calf Thymus DNA

r_0	ϕ (fixed) (deg)	K_s (dyne cm) $\times 10^{-12}$	P/D	τ_1 (ns)	f_1	τ_2 (ns)	χ^2
0.375	45	3.9	380	4.00			0.57
0.379	45	3.9	180	4.00			0.55
0.310	45	3.7	54	2.54			0.46
0.321	45	3.4	25	3.59	0.62	2.08	0.24

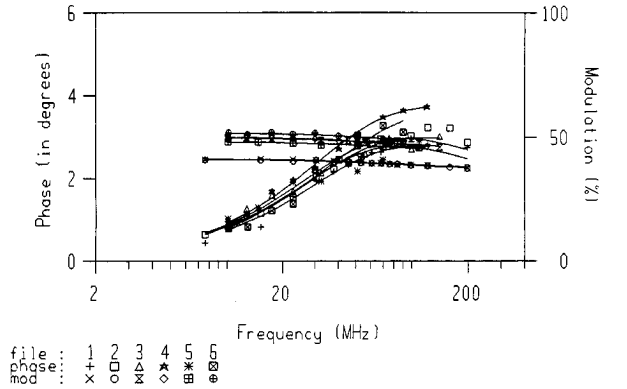

FIGURE 10: Result of the fit of the phase and modulation data using the flexible rod model and the energy transfer expressions for calf thymus DNA and for the ColE1 plasmid circular DNA. (1) Calf thymus P/D = 380, (2) P/D = 180, (3) P/D = 54, (4) P/D = 25, (5) ColE1 plasmid P/D = 45, (6) P/D = 16.

Table 6: Flexible Rod Model Analysis: ColE1 Plasmid DNA

r_0	ϕ (fixed) (deg)	K_s (dyne cm) $\times 10^{-12}$	P/D	τ_1 (ns)	f_1	τ_2 (ns)	χ^2
0.318	45	6.2	45	4.00	0.85	1.02	1.02
0.309	45	6.2	16	4.00	0.72	0.88	1.00

(b) DNA Results. Calf thymus DNA/DAPI complexes where studied in the P/D range from about 200 to about 2. At low P/D ratio, the intensity decay can be satisfactorily described using at least two exponential components or a continuous distribution of lifetime values. The results of the intensity decay fit for the double-exponential model are reported in Table 5 and Figure 10. Both decay models, namely, the double exponential and the continuous distribution of lifetime values, were used in the anisotropy decay fit. In this article, we report only the results using the double exponential models. The parameters of the fit, i.e., the angle ϕ and the spring constant K_s, were largely independent of the choice of the decay model. The anisotropy decay was analyzed using the flexible beads model as described in the theory section. The result of the fit for the ColE1 plasmid circular DNA are reported in Table 6 and also in Figure 10.

DISCUSSION

The dynamic model based on Schurr equation for the description of the anisotropy decay of a string of beads

satisfactorily describes the experimental results in the limit of very low DNA coverage, i.e., at very high P/D ratios. However, the mathematical form of the equation that describes the anisotropy decay does not allow an independent determination of the angle of the transition dipole moment of DAPI with the helix axis and of the spring constant. The correlation between the two parameters is such that they almost exactly compensate for a large range of angles. The value of the spring constant can vary from almost zero to about 13×10^{-12} dyn·cm provided that the angle ϕ compensates for the effective depolarizing motion. To explain this effect, a large depolarization can be obtained in two different ways: either by a stiff spring constant and an orientation of the DAPI molecule that projects a large depolarization on the helix axis or by a soft spring but a small angular projection. To resolve this ambiguity, we have used the homotransfer effect among DAPI molecules. We stress here that the measurement of the depolarization arising from the energy transfer term is essential for the determination of the orientation of the DAPI molecule and, then, the spring constant.

There is one particular orientation of the DAPI molecule in the minor groove which results in very low energy transfer efficiency to the next neighbor, i.e., the location four bases apart. If dye molecules can only be located at every four bases, then the next DAPI molecule can be located eight bases away from the first, at full coverage. Also, in this position, the energy transfer efficiency is very small. As a result, a peculiar effect should arise at very high DNA coverage. At low P/D ratio, energy transfer should become inefficient. This failure of transfer at low P/D ratio is a critical function of DAPI orientation. The observation of high transfer efficiency at low P/D ratios has allowed us to exclude the possibility that the minimum distance between DAPI molecules is four bases. Only if the dyes are located three bases apart can we explain the high transfer observed at high DNA coverage. We stress that the low polarization observed at low P/D ratio is a qualitative feature that can be directly observed from the data. This simple observation, which is independent of the complex model used for data analysis, provides very restrictive conditions regarding the location and orientation of DAPI molecules along the DNA helix. Since the amount of transfer also depends on the DAPI transition dipole moment orientation with respect to the helical axis, we have used the high coverage data set to determine the orientation of the DAPI molecule. Once the angle of the DAPI molecule is determined with respect to the helical axis, the spring constant can be obtained with precision. In the analysis of the anisotropy decay, it was also essential to fit all experiments simultaneously.

One important discussion concerns the errors in the parameters reported in Tables 1 and 3. Essentially, we have fit only one parameter, the angle ϕ. The value of K_s is dependent upon the value of ϕ. The standard deviation for the angle ϕ given by the Globals Unlimited fitting program is about 0.5°, when the other parameters are fixed. We should be cautious in using this figure for the uncertainty of ϕ, even in the presence of the relatively low reduced χ^2 obtained. To obtain the global fit, we have proceeded by steps: (1) In the limit of high P/D we have found the correlation between ϕ and K_s. (2) In the limit of low P/D, the value of ϕ can be determined very accurately only at full coverage. However, at full coverage, we have two additional effects that decrease our confidence in the determination of ϕ, namely, multiple transfer and the fluorescence contribution of the free dye. The extent of multiple transfer depends in turn on the intrinsic rate of transfer K_T and the distance of DAPI from the helix axis. The rate of transfer is relatively well defined by the overlap integral, but the distance at which we have placed the DAPI molecule from the DNA axis (8 Å) is somewhat arbitrary. From the above discussion, it appears that the correlation with the K_s parameter makes it problematic to establish the effective uncertainty of the angle ϕ. We have established the confidence interval for the angle ϕ on the basis of a series of considerations. At low P/D, the limiting value of the steady-state anisotropy is in the range 0.07−0.08. The low frequency limit of the low P/D data corresponds to an anisotropy of about 0.08, but this value is increased by the contribution of the free dye. The free dye, due to the short lifetime (0.15 ns) has a relatively large anisotropy (0.20). Therefore, the value of the steady-state anisotropy at full coverage depends on our evaluation of the contribution of the free dye, rather than on the determination of the steady-state value, which was obtained with high precision. The orientation of the transition dipole moment of DAPI that gives this range of the steady-state anisotropy is between 40° and 50° (Figure 8). The 45° value for ϕ is compatible with all the dynamic and steady-state data. On the basis of the above discussion, our maximum estimate for the range of the ϕ angle is $45° \pm 5°$.

The values of the structural parameters obtained from the fluorescence measurements are in excellent agreement with the crystal structure, determined by Dickerson and coworkers, of a dodecamer complexed with DAPI in the central AATT region, lying deep within the narrow groove (Larsen et al., 1989). In particular the angle of the DAPI molecule calculated from their deposited structure is 42°. Of course the spring constant cannot be obtained from the X-ray data. Previous determination of the spring constant by Allison and Schurr (1979) and Collini et al. (1992) are in the same range of values found in this study. We already noticed that the spring constant and the angle between the dye molecule and the DNA axis are not independent. The previous determinations of the spring constant are therefore dependent upon the assumed values of this angle. For ethidium bound to DNA, there is no full agreement about the value of this angle, due to the modification of the DNA structure by the intercalation of the ethidium dye. As a consequence, the value of the spring constant obtained in previous studies should be changed if this angle is changed due to a better determination of the structure of the complex.

The contribution to depolarization due to energy transfer was crucial for the determination of DAPI orientation and of the spring constant. Energy transfer depends on DNA coverage, which in turn depends on the modalities of DAPI−DNA binding. Given a certain mechanism for binding, both the concentration of DNA and of DAPI determine the exact coverage. Different depolarization regimes can be obtained depending on the DNA coverage. We have been able to observe different regimes, giving further confidence on the model employed. In the case of natural DNA, the relative abundance of particular sequences can influence the energy transfer contribution. The model we have employed for calculation of gap distributions assumes total randomness in the location of the bases, of course taking into account the AT/GC ratio of calf thymus DNA. However, if the distribution of AT pairs is not random, the contribution to

transfer can be erroneously estimated, which in turn influences the value of the spring constant calculated for the natural DNA. In particular a sequence of six AT pairs can give a large depolarization due to transfer at low P/D ratios, while a sequence of three AT pairs separated by one or two GC pairs will provide minimum depolarization due to transfer. Since after 9−10 base pairs the transfer is very small due to the large distance, we sample mostly AT pairs separated by one or two GC pairs. If the statistics of this sequence are different from that calculated assuming a random distribution of AT pairs, then our results, namely, the determination of the spring constant of the natural DNA, will also be affected.

The values obtained for the elastic spring constant of the Schurr model are different for the different polymers we have investigated. We stress once again that the spring constant cannot be obtained independently of the angle ϕ. Therefore, all the following discussion based on the assumption that this angle is the same for all DNAs and can very well be changed by assuming that the spring constant is the same, and that the angle can vary in the different complexes. With this clarification, we note that, among the synthetic polymers, the self-complementary is about a factor of 3 stiffer than the alternating. Instead, between the two natural DNAs we have investigated, the circular DNA is stiffer than the linear DNA. Calf thymus DNA is less stiff than the self-complementary double-stranded polymer but stiffer than the alternating one. However, inspection of eqs 1 reveals that we can only determine the product of γ and K_s. If the volume of the rotating bead is larger then γ will be larger, and the value of the spring constant would be smaller. In the case of the DAPI/DNA complex, we believe that the complex spans at least three bases and that the local rotating mass should be larger by at least a factor of 3. If we account for this mass factor, our estimations of the spring constant are in the same range of previous reported values based on the ethidium/DNA complex.

REFERENCES

Allison, S. A., & Schurr, J. M. (1979) Torsion dynamics and depolarization of fluorescence of linear macromolecules. I. Theory and application to DNA, *Chem. Phys. 41*, 35−44.

Barcellona, M. L., & Gratton, E. (1989) Fluorescence lifetime distributions of DNA/4′,6′-diamidine-2-phenylindole complex, *Biochim. Biophys. Acta 993*, 174−178.

Barcellona, M. L., & Gratton, E. (1990) The fluorescence properties of a DNA probe: 4′,6-diamidine-2-phenylindole (DAPI), *Eur. Biophys. 17*, 315−323.

Barcellona, M. L., & Gratton, E. (1991) A molecular approach to 4′,6-diamidine-2-phenylindole (DAPI) photophysical behavior at different pH values, *Biophys. Chem. 40*, 223−229.

Barcellona, M. L., & Gratton, E. (1993) Evidence for fluorescence energy homo-transfer occurring in DNA/DAPI complexes, *Med. Biol. Environ. 21*, 572−578.

Barcellona, M. L., Favilla, R., Von Berger, J., Avitabile, M., Ragusa, N., & Masotti, L. (1986) DNA/4′,6′-diamidine-2-phenylindole interactions. A comparative study employing fluorescence and ultraviolet spectroscopy, *Arch. Biochem. Biophys. 250*, 48−53.

Beecham, J. M., & Gratton, E. (1988) Fluorescence spectroscopy data analysis environment: A second generation global analysis program. Time resolved laser spectroscopy in biochemistry, *Proc. SPIE 909*, 70−81.

Beechem, J. M., Knutson, J. R., Ross, J. B. A., Turner, B. W., & Brand, L. (1983) Global resolution of heterogeneous decay by phase/modulation fluorometry: mixtures and proteins, *Biochemistry 22*, 6054−6058.

Burckhardt, G., Zimmer, C., & Luck, G. (1976a) Conformation and reactivity of DNA in the complex with protein IV. Circular dichroism of poly-a-histidine model complex with DNA polymers and specificity of the interaction, *Nucleic Acids Res. 3*, 561−580.

Burckhardt, G., Zimmer, C., & Luck, G. (1976b) Conformation and reactivity of DNA in the complex with protein III. Helix coil transition and conformational studies of model complexes of DNA's with poly-a-histidine, *Nucleic Acids Res. 3*, 537−559.

Cavatorta, P., Masotti, L., & Szabo, A. G. (1985) A time-resolved fluorescence study of 4′,6′-diamidine-2-phenylindole dihydrochloride binding to polynucleotides, *Biophys Chem. 22*, 11−16.

Champoux, J. J. (1978) Strand separation and the swivel in DNA replication, *Annu. Rev. Biochem. 47*, 449−479.

Chen, A. Y., Yu, C., Bodley, A., Peng, L. F., & Liù, L. F. (1993) A new mammalian DNA Topoisomerase-I poison HOECHST-33342-cytotoxicity and drug resistance in human cell cultures, *Cancer Res. 53*, 1332−1337.

Clegg, R. M., Murchie, A. I. M., Zechel, A., Carlberg, C., Diekman, S., & Lilley, D. M. J. (1992) Fluorescence resonance energy-transfer analysis of the structure of the four-way DNA junction, *Biochemistry 31*, 4846−4856.

Clegg, R. M., Murchie, A. I. M., Zechel, A., & Lilley, D. M. J. (1993) Observing the helical geometry of double-stranded DNA in solution by fluorescence resonance energy-transfer, *Proc. Natl. Acad. Sci. U.S.A. 90*, 2994−2998.

Clegg, R. M., Murchie, A. I. H., & Lilley, D. M. J. (1994) The solution structure of the four-way DNA junction at low-salt conditions. A fluorescence resonance energy transfer analysis, *Biophys J. 66*, 99−109.

Collini, M., Chirico, G., & Baldini, G. (1992) DNA torsion dynamics by multifrequency phase fluorometry, *Biopolymers 32*, 1447−1459.

Cooper, J. P., & Hagerman, P. J. (1990) Analysis of fluorescence energy transfer in duplex and branched DNA molecules, *Biochemistry 29*, 9261−9268.

Dervan, P. B. (1986) Design of sequence-specific DNA-binding molecules, *Science 232*, 464−471.

Dickman, S., Hillen, W., Morgeneyer, B., Wells, R. D., & Porschke, D. (1982) Orientation relaxation of DNA restriction fragments and the internal mobility of the double helix, *Biophys. Chem. 15*, 263−270.

Eis, P. S., & Millar, D. P. (1993) Conformational distributions of a four-way DNA junction revealed by time-resolved fluorescence energy transfer, *Biochemistry 32*, 13852−13860.

Eriksson, S., Kim, S. K., Kubista, M., & Norden, B. (1993) Binding of 4′,6-diamidino-2-phenylindole (DAPI) to AT regions of DNA: evidence for an allosteric conformational change, *Biochemistry 32*, 2987−2998.

Förster, T. (1951) Energy transfer. Fluorescenz organischer Verbindungen. *Gottingen 22*, 61−83.

Fujimoto, B. S., Shibata, J. H., Schurr, R. L., & Schurr, J. M. (1985) Torsional dynamics and rigidity of fractionated poly (dGdC), *Biopolymers 24*, 1009−1022.

Ginell, S., Lessinger, L., & Burman, H. M. (1988) The crystal and molecular structure of the anticancer drug Actinomicin D; some explanations for its unusual properties, *Biopolymers 27*, 843−864.

Gratton, E., & Limkeman, M. (1983a) A continuously variable frequency cross-correlation phase fluorometer with picosecond resolution, *Biophys. J. 44*, 315−324.

Gratton, E., & Linkeman, M. (1983b) Microprocessor-controlled photon-counting spectrofluorometer, *Rev. Sci. Instrum. 54*, 294−299.

Gratton, E., Jameson, D. M., & Hall, R. (1984a) Multifrequency phase and modulation fluorometry, *Annu. Rev. Biophys. Bioeng. 13*, 105−124.

Gratton, E., Lakowicz, J. R., Maliwal, B., Cherek, H., Laczko, G., & Linkeman, M. (1984b) Resolution of mixtures of fluorophores using variable-frequency phase and modulation data, *Biophys J. 46*, 479−486.

Hard, T., Fan, P., & Kearns, D. R. (1990) A fluorescence study of the binding of Hoechst 33258 and DAPI to halogenated DNA, *Photochem. Photobiol. 51*, 77−86.

Hogan, M., Dattagupta, N., & Crothers, D. M. (1979) Transient electric dichroism studies of the structure of the DNA complex with intercalated drugs, *Biochemistry 18*, 280−288.

Jain, S. C., & Sobell, H. M. (1984) Structures of two ethidium-dinucleoside monophosphate crystalline complexes containing ethidium: cytidyl (3′-5′) guanosine, *J. Biomol. Struct. Dyn. 1*, 1179−1194.

Jansen, K., Lincoln, P., & Norden, B. (1993) Binding of DAPI analogue 2,5-Bis(4-amidinophenyl) furan to DNA, *Biochemistry 32*, 6605−6612.

Kahn, J. D., Yun, E., & Crothers, D. M. (1994) Detection of localized DNA flexibility, *Nature 368*, 163−166.

Kapuscinski, J., & Szer, W. (1979) Interactions of 4′,6′-diamidine-2-phenylindole dihydrochloride with synthetic polynucleotides, *Nucleic Acids Res. 6*, 3519−3534.

Kubista, M., Akerman, B., & Norden, B. (1987) Characterization of interaction between DNA and 4′,6-diamidino-2-phenylindole by optical spectroscopy, *Biochemistry 26*, 4545−4553.

Kubista, M., Akerman, B., & Norden, B. (1988) Induced circular dichroism in nonintercalative DNA−drug complexes. Sector rules for structural applications, *J. Phys. Chem. 92*, 2352−2356.

Kumar, S., Joseph, T., Singh, M. P., Bathini, Y., & Lown, Y. W. (1992) Analogs of Hoechst 33258-high field H-1-NMR and restrained molecular mechanics studies, *J. Biomol. Struct. Dyn. 9*, 853−880.

Lakowicz, J. R. (1986) in *Principles of fluorescence spectroscopy*, 3rd ed., pp 305−337, Plenum Press, New York and London.

Larsen, T. A. Goodsell, D. S., Cascio, D., Grzeskowiak, K., & Dickerson, R. E. (1989) The structure of DAPI bound to DNA, *J. Biomol. Struct. Dyn. 7*, 477−491.

Lilley, D. M. J., & Clegg, R. M. (1993) The structure of the 4-way junction in DNA, *Annu. Rev. Biophys Biomol. Struct. 22*, 299−328.

Loontiens, F. G., McLaughlin, L. W., Dickmann, S., & Clegg, R. M. (1991) Binding of Hoechst 33258 and 4′,6-diamidino-2-phenylindole to self-complementary decadeoxynucleotides with modified exocyclic base substituent, *Biochemistry 30*, 182−189.

Manzini, G., Barcellona, M. L., Avitabile, M., & Quadrifoglio, F. (1983) Interaction of 4′,6-diamidine-2-phenylindole (DAPI) with natural and synthetic nucleic acids, *Nucleic Acids Res. 11*, 8861−8875.

Manzini, G., Xodo, L., Barcellona, M. L., & Quadrifoglio, F. (1985a) Interaction of DAPI with synthetic and natural deoxy- and ribonucleic acids, *J. Biosci. 8*, 699−711.

Manzini, G., Xodo, L., Barcellona, M. L., & Quadrifoglio, F. (1985b) Interaction of DAPI with double-stranded ribonucleic acids, *Nucleic Acids Res. 13*, 8955−8967.

Masotti, M., Barcellona, M. L., Von Berger, J., & Avitabile, M. (1981) Fluorimetric detection of different structures induced by concentration changes of alkaline and alkaline-earth counterions on covalently closed DNA, *Biosci. Rep. 1*, 701−707.

Masotti, L., Cavatorta, P., Avitabile, M., Barcellona, M. L., & Ragusa, N. (1982) Characterization of 4′,6-diamidino-2-phenylindole (DAPI) as a fluorescent probe of DNA structure, *Ital. J. Biochem. 31*, 90−99.

Mathieson, A. R., & Olayemi, J. Y. (1975) The interaction of calcium and magnesium ions with deoxyribonucleic acid, *Arch. Biochem. Biophys. 169*, 237−243.

McGhee, J. D., & von Hippel, P. H. (1974) Theoretical aspects of DNA−protein interactions: co-operative and non-co-operative binding of large ligands to a one-dimensional homogeneous lattice, *J. Mol. Biol. 86*, 469−489.

Mergny, J. L., Boutorine, A. S., Garestier, T., Belloc, F., Rougee, M., Bulychev, N. V., Koshkin, A. A., Bourson, J., Lebedev, A. V., Valeur, B., Nguyen, T. T., & Helene, C. (1994) Fluorescence energy transfer as a probe for nucleic acid structures and sequences, *Nucleic Acids Res. 22*, 920−928.

Misra, V. K., Sharp, K. A., Friedman, R. A., & Honig, B. (1994) Salt effects on ligand−DNA binding minor groove binding antibiotics, *J. Mol. Biol. 238*, 245−263.

Mohan, S., & Yathindra, N. (1991) Flexibility of DNA in 2:1 drug DNA complexes-simultaneous binding of two DAPI molecules to DNA, *J. Biomol. Struct. Dyn. 9*, 695−770.

Neidle, S., Pearl, L. H., & Skelly, J. V. (1987) DNA structure and perturbation by drug binding, *Biochem. J. 243*, 1−13.

Ott, G. B., Ziegler, R., & Bauer, W. (1975) The DNA melting transitions in aqueous magnesium salt solutions, *Biochemistry 14*, 3431−3438.

Paoletti, J., & Le Pecq, J. B. (1971) Resonance Energy Transfer between Ethidium Bromide Molecules bound to Nucleic Acids, *J. Mol. Biol. 59*, 43−62.

Pjura, P. E., Grzeskowiak, K.., & Dickerson R. E. (1987) Binding of Hoechst 33258 to the minor groove of B-DNA, *J. Mol. Biol. 197*, 257−271.

Pullman, A., & Pullman, B. (1981) Molecular electrostatic potential of the nucleic acids, *Q. Rev. Biophys. 14*, 289−380.

Record, M. T. (1975) Effects of Na^+ and Mg^{2+} ions on the helix−coil transition of DNA, *Biopolymers 14*, 2137−2158.

Robinson, M. J., Corbett, A. H., & Osheroff, N. (1993) Effects of Topoisomerase II-targeted drugs on enzyme-mediated DNA cleavage of ATP hydrolysis: evidence for distinct drug interaction domains on Topoisomerase II, *Biochemistry 32*, 3638−3643.

Schurr, J. M. (1984) Rotational diffusion of deformable macromolecules with mean local cylindrical symmetry, *Chem. Phys. 84*, 71−96.

Schurr, J. M., & Fujimoto, B. S. (1988) The amplitude of local angular motions of intercalated dyes and bases in DNA, *Biopolymers 27*, 1543−1569.

Spink, N., Brown, D. G., & Neidle, S. (1994) Sequence-dependent effects in drug−DNA interaction: the crystal structure of Hoechst 33258 bound to the d(CGCAAATTTGCG) duplex, *Nucleic Acids Res. 22*, 1607−1612.

Storl, K., Burckhardt, G., Lown, J. W., & Zimmer, C. (1993) Studies on the ability of minor groove binders to induce supercoiling in DNA, *FEBS Lett. 334*, 49−54.

Syvanen, M. (1975) Processing of bacteriophage lambda DNA during its assembly into heads, *J. Mol. Biol. 91*, 165−174.

Szabo, A. G., Krajcarski, D. T., Cavatorta, P., Masotti, L., & Barcellona, M. L. (1986) Excited state pK_a behaviour of DAPI. A rationalization of fluorescence enhancement of DAPI in DAPI−nucleic acid complexes, *Photochem. Photobiol. 44*, 143−150.

Tanious, F., Veal, J., Buczak, H., Ratmeyer L. S., & Wilson, W. D. (1992) DAPI (4′,6-diamidino-2-phenylindole) binds differently to DNA and RNA: minor-groove binding at AT sites and intercalation at AU sites, *Biochemistry 31*, 3103−3112.

Tanious, F. A., Spychala, J., Kumar, A., Greene, K., Boykin, D. W., & Wilson, W.D. (1994) Different binding mode in AT and GC sequences for unfused-aromatic dications, *J. Biomol. Struct. Dyn. 11*, 1063−1083.

Thomas, J. C., Allison, S. A., Appellof, C. J., & Schurr, J. M. (1980) Torsion dynamics and depolarization of fluorescence of linear macromolecules. II. Fluorescence polarization anisotropy measurements on a clean viral 29 DNA, *Biophys. Chem. 12*, 177−188.

Wilson, W. D., Tanious, F. A., Barton, H. J., Strekowski, L., & Boykin, D. W. (1985a) Poly (dA)-Poly(dT) exists in an unusual conformation under physiological conditions: propidium binding to poly (dA)-poly (dT) and poly d(A-T)-poly d(A-T), *Biochemistry 24*, 3991−3999.

Wilson, W. D., Krishnamoorthy, C. R., Wang, Y. H., & Smith, J. C. (1985b) Mechanism of intercalation: ion effects on the equilibrium and kinetic constants for the interaction of propidium and ethidium with DNA, *Biopolymers 24*, 49−55.

Wilson, W. D., Tanious, F. A., Barton, H. J., Strekowski, L., & Boykin, D. W. (1989) Binding of 4′,6-diamidino-2-phenylindole (DAPI) to GC and mixed sequences in DNA: intercalation of a classical groove-binding molecule, *J. Am. Chem. Soc. 111*, 5008−5010.

Wilson, W. D., Tanious, F. A., Barton, H. J., Jones, R. L., Fox, K., Widra, R. L., & Strekowski, L. (1990) DNA sequence dependent binding modes of 4′,6-diamidino-2-phenylindole (DAPI), *Biochemistry 29*, 8452−8461.

Wolf, B., Berman, S., & Hanlon, S. (1977) Structural transitions of calf thymus DNA in concentrated LiCl solutions, *Biochemistry 16*, 3655−3662.

Wu, P. G., Fujimoto, L. S., & Schurr, J. M. (1991) Effect of ethidium on the torsion constants of linear and supercoiled DNAs, *Biophys. Chem. 41*, 217−236.

Zimmer, C., & Waehnert, U. (1986) Nonintercalating DNA-binding ligands: specificity of the interaction and their use as tools in biophysical biochemical and biological investigations of the genetic material, *Prog. Biophys. Mol. Biol. 47*, 31−112.

BI951027B